Circulation

American Heart Association®

Learn and Live℠

Chronic Unloading by Left Ventricular Assist Device Reverses Contractile Dysfunction and Alters Gene Expression in End-Stage Heart Failure

Paul M. Heerdt, Jeffrey W. Holmes, Bolin Cai, Alessandro Barbone, John D. Madigan, Steven Reiken, David L. Lee, Mehmet C. Oz, Andrew R. Marks and Daniel Burkhoff

The online version of this article, along with updated information and services, is located on the World Wide Web at:

http://circ.ahajournals.org/cgi/content/full/102/22/2713

Chronic Unloading by Left Ventricular Assist Device Reverses Contractile Dysfunction and Alters Gene Expression in End-Stage Heart Failure

Paul M. Heerdt, MD, PhD; Jeffrey W. Holmes, MD, PhD; Bolin Cai, MD, PhD;
Alessandro Barbone, MD; John D. Madigan, BA; Steven Reiken, PhD; David L. Lee, MD;
Mehmet C. Oz, MD; Andrew R. Marks, MD; Daniel Burkhoff, MD, PhD

Background—Left ventricular (LV) assist devices (LVADs) can improve contractile strength and normalize characteristics of the Ca^{2+} transient in myocytes isolated from failing human hearts. The purpose of the present study was to determine whether LVAD support also improves contractile strength at different frequencies of contraction (the force-frequency relationship [FFR]) of intact myocardium and alters the expression of genes encoding for proteins involved in Ca^{2+} handling.

Methods and Results—The isometric FFRs of LV trabeculae isolated from 15 patients with end-stage heart failure were compared with those of 7 LVAD-supported patients and demonstrated improved contractile force at 1-Hz stimulation, with reversal of a negative FFR after LVAD implantation. In 20 failing hearts, Northern blot analysis for sarcoplasmic endoreticular Ca^{2+}-ATPase subtype 2a (SERCA2a), the ryanodine receptor, and the sarcolemmal Na^+-Ca^{2+} exchanger was performed on LV tissue obtained before and after LVAD implantation. These paired data demonstrated an upregulation of all 3 genes after LVAD support. In tissue obtained from subsets of these patients, Western blot analysis was performed, and oxalate-supported Ca^{2+} uptake by isolated sarcoplasmic reticular membranes was determined. Despite higher mRNA for all genes after LVAD support, only SERCA2a protein was increased. Functional significance of increased SERCA2a was confirmed by augmented Ca^{2+} uptake by sarcoplasmic reticular membranes isolated from LVAD-supported hearts.

Conclusions—LVAD support can improve contractile strength of intact myocardium and reverse the negative FFR associated with end-stage heart failure. The expression of genes encoding for proteins involved in Ca^{2+} cycling is upregulated (reverse molecular remodeling), but only the protein content of SERCA2a is increased. (*Circulation*. 2000;102:2713-2719.)

Key Words: heart failure ■ sarcoplasmic reticulum ■ calcium ■ genes ■ heart-assist device

---

Recent evidence indicates that left ventricular (LV) assist device (LVAD) support in patients with end-stage heart failure can lead to normalization of heart structure and improved intrinsic myocyte strength.[1–6] These observations have led to the notion that LVADs may be used to normalize heart function in some patients,[7] thus obviating the need for transplantation. However, current understanding of the scope and mechanisms of this recovery is limited.

Myocardial contractile dysfunction in heart failure due to a variety of causes has been linked to alterations in Ca^{2+} cycling.[8,9] Downregulated gene expression of sarcoplasmic endoreticular Ca^{2+}-ATPase subtype 2a (SERCA2a) and of the sarcoplasmic reticular (SR) ryanodine-sensitive Ca^{2+} release channel (ryanodine receptor [RyR]) and altered regulation of the sarcolemmal Na^+-Ca^{2+} exchanger have been reported and appear to correlate with various aspects of contractile dysfunction.[10–14] Recent studies of isolated myocytes have demonstrated LVAD-induced recovery of contractile strength in

unloaded cells that coincides with the normalized magnitude and time course of the intracellular Ca^{2+} transient.[3] Accordingly, we hypothesized that LVAD support would also improve the contractile strength of intact failing myocardium and upregulate the expression of genes encoding for Ca^{2+}-cycling proteins. To test this hypothesis, we analyzed how prolonged LVAD support influenced the contractile properties of isometric LV trabeculae at different stimulation rates and the expression of genes encoding for SERCA2a, RyR, and the Na^+-Ca^{2+} exchanger.

Methods

Patient Population and LVAD Implant

Under a protocol approved by the Institutional Review Board of the New York Presbyterian Hospital, LV myocardium obtained from 47 patients with end-stage heart failure (CHF hearts) and from 3 nonfailing hearts was used for the study. Of the CHF hearts, 27 had been supported with an LVAD (CHF+LVAD). The 3 nonfailing

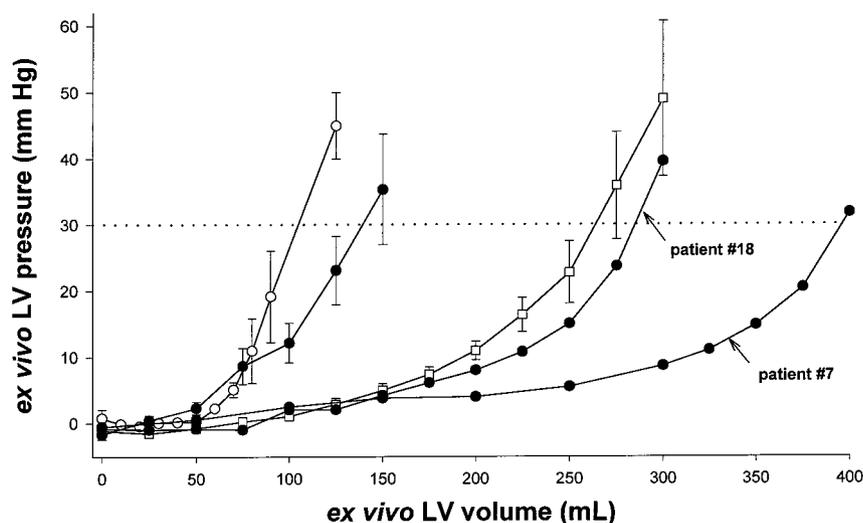*Circulation* is available at http://www.circulationaha.org

Figure 1. Ex vivo LV pressure-volume relationships from explanted hearts. Open circles indicate mean±SEM of 3 nonfailing hearts; open squares, mean±SEM of 8 non-LVAD CHF hearts; and closed circles, mean±SEM of 9 LVAD-supported hearts. Curves for 2 hearts supported with malfunctioning LVAD are designated by patient numbers corresponding to those on Table 1. Dotted line designates pressure of 30 mm Hg.

hearts were unsuitable for transplantation because of hepatitis B, extensive atrial damage during harvest, and high creatine phosphokinase levels with subsequently normal MB fraction, respectively. For LVAD patients, insertion and operation of the device (Thermo Cardio Systems Inc) were performed as previously described.[2] Inflow to the LVAD is provided through a conduit inserted into the LV via an ≈1-in hole in the apex. Tissue removed in making this hole was immediately frozen in liquid nitrogen and subsequently used for pre-LVAD biochemical and molecular analyses and/or immersed in iced Krebs' solution for measurement of trabecular force production and the force-frequency relationship (FFR, detailed below).

Heart Explantation and LV Pressure-Volume Relationships

At the time of transplantation, all hearts were perfused with 4°C hypocalcemic hyperkalemic cardioplegia solution, and tissue samples were obtained with the heart cold. Before tissue harvest in 3 nonfailing, 8 CHF, and 10 CHF+LVAD patients, the hearts were subjected to analysis of static LV pressure-volume relationships as described previously.[1] Briefly, with the heart kept cold, pressure within a compliant water-filled latex balloon in the LV chamber was measured with a high-fidelity micromanometer while volume was progressively increased. The pressure was plotted as a function of volume at each step, resulting in static LV pressure-volume relationships. To index LV structure for comparison between hearts, the volume at a pressure of 30 mm Hg (V_{30}) was determined.

Myocardial Force Generation at Different Stimulation Frequencies

FFR data were obtained from free wall trabeculae isolated from 1 nonfailing heart, 15 CHF hearts, 5 pre-LVAD core samples, and 7 post-LVAD hearts; trabeculae were isolated from both pre- and post-LVAD tissue in 3 of the LVAD patients. From all tissue samples, trabeculae <1 mm in diameter were excised and immersed in ice-cold Krebs-Ringer solution with 30 mmol/L 2,3-butanedione monoxime before mounting in a bath with one end connected to a force transducer and the other connected to a micrometer. During superfusion with 37°C oxygenated Krebs-Ringer solution (rate 1 mL/min, bath volume 1 mL), trabeculae were stimulated at 1 Hz and allowed to equilibrate for at least 1 hour at slack length. The trabeculae were then progressively stretched to the length of maximal force generation. After reequilibration, the stimulation frequency was increased every 5 minutes at 0.5-Hz increments to a maximum of 2.5 Hz (150 bpm). For each preparation, force development at increasing stimulation frequency was referenced to the baseline level at 1 Hz.

Northern Blot Analysis

In 20 patients, tissue was obtained both before LVAD (apical core) and after LVAD (free wall) for Northern blot analysis. Apical and free wall tissue samples obtained from 8 non-LVAD CHF hearts were also analyzed to determine whether regional differences in gene expression exist. For all samples, only tissue without gross evidence of infarction or scarring was analyzed. Total RNA was extracted from myocardium with guanidinium thiocyanate, followed by centrifugation in cesium chloride solutions. Aliquots of total RNA were then separated by electrophoresis, transferred to nitrocellulose membranes, and then hybridized with cDNA for rat SERCA2a (1.181-kb *Eco*RI fragment), the human Na^+-Ca^{2+} exchanger (0.659-kb *Eco*RI-*Pst*I fragment), rabbit RyR (0.55-kb *Eco*RI-*Bam*HI fragment), and human GAPDH (1.3-kb *Pst*I fragment). All cDNA probes were labeled with [^{32}P]dCTP (3000 Ci/mmol, Amersham) to a specific activity of 1×10^6 cpm/μg by use of a multiprimer DNA labeling system (Amersham). The blots were exposed to X-OMAT AR film, and autoradiograms were then analyzed by laser densitometry in the linear response range of the x-ray films with GAPDH used as an internal standard. The relative expression of each gene was quantified as the ratio of target band intensity to GAPDH band intensity standardized to the average of nonfailing samples on the blot. The same nonfailing hearts were used for standardization with a value of 1 arbitrarily designated as normal.

Western Blot Analysis

In 4 patients, sufficient myocardium was obtained from the pre-LVAD apical core to allow for both mRNA isolation and Western blot analysis for target proteins. These data were then compared with similar analysis of post-LVAD free wall from the same hearts. For Western blot, ≈1 g of tissue was homogenized in 1.0 mL of ice-cold buffer containing 20 mmol/L Na-HEPES, pH 7.4, 4.0 mmol/L EGTA, 1.0 mmol/L dithiothreitol, and EDTA-free complete protease inhibitors (Boehringer-Mannheim). Samples were centrifuged, and protein concentration of the supernatant was determined before SDS-PAGE by using 6% gels to detect RyR and 7.5% gels to detect SERCA2a and the Na^+-Ca^{2+} exchanger. Proteins were immediately transferred to nitrocellulose and then blocked by incubation with 5% nonfat dry milk in Tris-buffered saline (TBS) containing 0.1% Tween 20 (TBS-T buffer). After they were washed with TBS-T buffer, the blots were incubated with primary antibody for 1 hour. Primary antibodies were diluted in 5% nonfat dry milk in TBS-T buffer and included an anti-RyR antibody[15] (1:3000 dilution), a mouse monoclonal antibody against SERCA2a (Novocastra Laboratories Ltd, diluted 1:500), and an anti–Na^+-Ca^{2+} exchanger antibody (Swant, diluted 1:1000). After washes with TBS-T buffer, membranes were incubated with peroxidase-conjugated goat anti-rabbit or goat anti-mouse IgG antiserum (Boehringer-Mannheim) diluted

TABLE 1.   Patient Data

Patient	Disease	Sex	Age, y	EF, %	LVAD Duration, d	LVAD Function	Medications/Interventions Implant	Explant
1	DCM (ethanol)	M	57	16	48	Normal	DOB, DA, NE, furosemide	Captopril, furosemide
2	DCM (familial)	M	56	18	116	Normal	DOB, DA, NE, bumetaninde	Captopril, furosemide
3	DCM (idiopathic)	M	54	20	24	Normal	DOB, DA, MIL, furosemide	
4	DCM (idiopathic)	M	49	33	63	Normal	DA, MIL, VASOP	Captopril, furosemide
5	DCM (idiopathic)	M	35	15	93	Normal	DOB, DA, MIL, amiodarone	Amiodarone
6	DCM (idiopathic)	M	64	15	99	Normal	DOB, DA, MIL, amiodarone, digoxin	Amiodarone
7	DCM (idiopathic)	M	18	15	108	Inflow obstruction	DOB, DA, MIL, amiodarone	Captopril
8	DCM (myocarditis)	M	18	15	148	Normal	DOB, DA, MIL, furosemide	Digoxin
9	DCM (postpartum)	F	37	18	106	Normal	DOB, MIL, bivad	Lisinopril, digoxin
10	DCM (viral)	M	31	16	77	Normal	DOB, DA	
11	DCM/ICM (idiopathic)	M	50	15	60	Normal	DOB, DA, NE, IABP	
12	ICM	F	50	14	151	Normal	NE, digoxin, furosemide	
13	ICM	M	63	18	92	Normal	DOB, MIL, NE, TNG	Captopril, furosemide, digoxin
14	ICM	M	65	20	33	Normal	DOB, DA	Captopril, furosemide, digoxin
15	ICM	M	53	22	86	Normal	DOB, DA, MIL, NE, VASOP, IABP	Amiodarone
16	ICM	M	60	20	50	Normal	DA, MIL, NE, digoxin, furosemide	Digoxin
17	ICM	M	64	17	83	Normal	DOB, DA, amiodarone, IABP	
18	ICM	M	62	25	142	Inflow regurgitation	DOB, DA, MIL, nitroprusside	
19	ICM (acute MI)	M	56	10	128	Normal	DA, MIL, NE, VASOP, LIDO, IABP	Captopril
20	ICM (postcardiotomy)	M	64	15	60	Normal	DOB, MIL, TNG, amiodarone	Amiodarone, captopril
Mean±SEM			50±3	18±1	88±9			

EF indicates ejection fraction; DOB, dobutamine; DA, dopamine; NE, norepinephrine; MIL, milrinone; VASOP, vasopressin; bivad, biventricular assist device; TNG, trinitroglycerine; IABP, intra-aortic balloon pump; and LIDO, lidocaine.

1:3000, washed with TBS-T buffer, and developed with the use of ECL (Amersham Pharmacia Biotech).

SR Preparation

Ca^{2+} uptake by SR membranes isolated from 2 nonfailing, 5 CHF, and 4 CHF+LVAD hearts was directly assayed by use of the suction filtration method[16] adapted to eliminate the regulatory effects of phospholamban by providing a relative excess of Ca^{2+}. Briefly, after tissue homogenization, membrane vesicles enriched in SR were isolated by sequential centrifugation, resuspended in sucrose/histidine, and placed in uptake medium (50 mmol/L histidine, 3 mmol/L $MgCl_2$, 100 mmol/L KCl, 5 mmol/L potassium oxalate, and 0.05 mmol/L $CaCl_2$ with tracer $^{45}Ca^{2+}$). After incubation, Ca^{2+} uptake was initiated by the addition of 3 mmol/L ATP. Before and 5 minutes after ATP administration, aliquots were removed and analyzed for protein and ionized Ca^{2+} by spectrophotometry with 1,2-bis(2-aminophenoxy)ethane-N,N,N′,N′-tetraacetic acid as the Ca^{2+} indicator. Aliquots were then suctioned through a 0.45-μm filter and washed with KCl, imidazole, EGTA, and $MgCl_2$. Radioactivity of the filtrate and the filter was then counted, and Ca^{2+} uptake in terms of nanomoles per liter per milligram protein was calculated. For each heart, Ca^{2+} uptake was measured in both the absence and presence of 300 μmol/L ryanodine, and the difference between measurements was used to index the contribution of RyR to Ca^{2+} flux across the membrane.

Statistical Analysis

All pre- and post-LVAD data from the same patient were compared by paired *t* test, as were apical and free wall mRNA data from the same heart. Comparisons between groups were made by ANOVA. For all tests, a value of $P \leq 0.05$ was considered significant.

Results

Hemodynamic Effects of LVAD Support

Characteristics of patients from whom pre- and post-LVAD tissue samples were obtained are shown in Table 1, with patients subdivided under the broad categories of dilated (DCM) or ischemic (ICM) cardiomyopathy. The duration of LVAD support ranged from 24 to 151 days. Two patients exhibited echocardiographic evidence of LVAD valvular malfunction: one with inflow obstruction (patient 7) and the other with inflow regurgitation (patient 18). Hemodynamic variables, which were obtained with the patients anesthetized and mechanically ventilated before LVAD implantation and with the patients receiving full LVAD support immediately before heart transplant, are shown in Table 2.

Static LV Pressure-Volume Relationships

Ex vivo pressure-volume relationships are shown in Figure 2. A marked difference between the nonfailing and CHF hearts is evident, with the curve derived from the CHF+LVAD hearts falling between these 2 extremes. Mean V_{30} values for the nonfailing and CHF+LVAD hearts were not significantly different (96±10 and 138±11 mL, respectively), whereas the mean V_{30} value for the CHF hearts (267±20 mL) was greater than the values for the others ($P<0.001$). Consistent with a previous report,[17] the pressure-volume relationships of the 2

TABLE 2.   Hemodynamic Data Before and During LVAD Support

	LVAD Support	
	Before	During
HR, bpm	88±3	72±4*
CI, L · min^{-1} · m^{-2}	1.8±0.1	2.4±0.1*
CVP, mm Hg	16±2	9±1*
mPAP, mm Hg	37±2	17±1*
PCWP, mm Hg	25±2	8±1*
mAP, mm Hg	71±3	78±2

Values are mean±SEM. HR indicates heart rate; CI, cardiac index; CVP, central venous pressure; mPAP, mean pulmonary arterial pressure; PCWP, pulmonary capillary wedge pressure; and mAP, mean arterial pressure.

*$P \le 0.05$ vs before LVAD support.

hearts with LVAD inflow valve dysfunction (patients 7 and 18) were similar to those of the CHF hearts not receiving LVAD support.

Trabecular FFRs

Trabecular dimensions were similar among all groups, as was developed force at 1 Hz in trabeculae from pre-LVAD core samples and the free wall of non-LVAD hearts (Table 3). In contrast, developed force at 1 Hz in trabeculae isolated from the LV free wall of post-LVAD hearts tended to be higher than that measured in pre-LVAD core trabeculae, although with the small sample size, this difference did not achieve statistical significance. Developed force was reduced similarly by increasing stimulation frequency in the pre-LVAD core and non-LVAD transplant samples but, on average, did not decline in the post-LVAD samples (Figure 2A). Representative force tracings from individual hearts are shown in Figure 2C. The effects of increased stimulation frequency on developed force in the 3 paired pre-LVAD and post-LVAD trabeculae are summarized in Figure 2B, which suggests that in individual hearts, LVAD support converts the FFR from negative to positive.

Northern Blot Analysis

In non–LVAD-supported CHF hearts (Figure 3), apical SERCA2a mRNA levels were, on average, greater than in the free wall, whereas RyR and the Na$^+$-Ca^{2+} exchanger mRNA were not different. A representative Northern blot depicting pre- and post-LVAD samples obtained from the same hearts is shown in Figure 4. The normalized pre- and post-LVAD mRNA values for all patients are shown in Figure 5. mRNA

TABLE 3.   LV Trabecular Data

Parameter	CHF (No LVAD) Free Wall	Pre-LVAD Core Tissue	Post-LVAD Free Wall
Diameter, mm	0.85±0.03	0.80±0.07	0.80±0.10
Length, mm	4.4±0.40	3.9±0.84	5.6±0.78
Mass, g	2.6±0.29	1.8±0.20	3.1±0.73
Cross-sectional area, mm^2	0.57±0.04	0.52±0.09	0.55±0.15
Developed force (1 Hz), g/mm^2	8.4±1.0	9.2±2.0	12.7±3.3

levels of SERCA2a, RyR, and the Na$^+$-Ca^{2+} exchanger were higher in the post-LVAD free wall than in the pre-LVAD apex. Statistical analysis failed to show any correlation between post-LVAD mRNA values for any of the genes and the duration of LVAD support, patient age, the value of any hemodynamic parameter, or V$_{30}$.

SERCA2a, RyR, and Na$^+$-Ca^{2+} Exchanger Protein

A Western blot of protein obtained from 4 paired pre- and post-LVAD samples and 1 nonfailing heart is shown in Figure 6. Semiquantitative densitometric analysis with values standardized to those measured in the nonfailing heart demonstrated, on average, no change in RyR (71±3% versus 91±16%, $P=0.06$) and the Na$^+$-Ca^{2+} (116±16% versus 112±12%, $P=0.6$) exchanger protein but an ≈4-fold increase (15±14% versus 62±8%, $P=0.001$) in SERCA2a.

SR Ca^{2+} Uptake

The amount of oxalate-supported Ca^{2+} uptake over 5 minutes was 394±42 nmol/L per milligram protein for nonfailing hearts, 296±20 nmol/L per milligram protein for CHF hearts, and 372±51 nmol/L per milligram protein for CHF+LVAD hearts. The addition of ryanodine to the incubation medium to block concomitant release via the RyR increased Ca^{2+} uptake by 25% in nonfailing membranes but only by 10% in SR membranes from both CHF and CHF+LVAD hearts.

Discussion

In some patients, LVAD support leads to sufficient improvement in global pump function for explant of the device.[7,18] Although long-term outcome has been poor in many patients,[18,19] the concept that LVADs may have a role as a "bridge to recovery" has developed, in part, because of studies demonstrating reversal of chamber enlargement, reduction in LV mass, and regression of myocyte hypertrophy.[1,4,5,20] In addition, recent data showing an increased rate of unloaded myocyte shortening,[3] an enhanced inotropic response to β-adrenergic stimulation,[3,21] and improved cytosolic Ca^{2+} transients (increased peak, accelerated decay)[3] after LVAD serve to underscore the multitude of abnormalities that may undergo recovery, even in severely diseased myocardium.

The finding of LVAD-induced improvement in isolated myocyte Ca^{2+} metabolism is of particular interest because under most circumstances of severe heart failure, myocardial systolic and diastolic contractile dysfunction are associated with abnormal excitation-contraction coupling.[8,9] Recent data have demonstrated increased SERCA2a protein after LVAD support,[22] but whether the contractile strength of intact myocardium also improves remained unknown. Consistent with prior studies,[14,23] the present study revealed a negative FFR in trabeculae isolated from failing hearts. Importantly, the behaviors of free wall tissue obtained from non-LVAD transplant hearts and apical tissue obtained at the time of LVAD implantation were similar, thus excluding the possibility that regional factors contributed to differences between these pre- and post-LVAD data. After LVAD support, force at all stimulation rates tended to increase, and the FFR in individual hearts was converted from negative to positive.
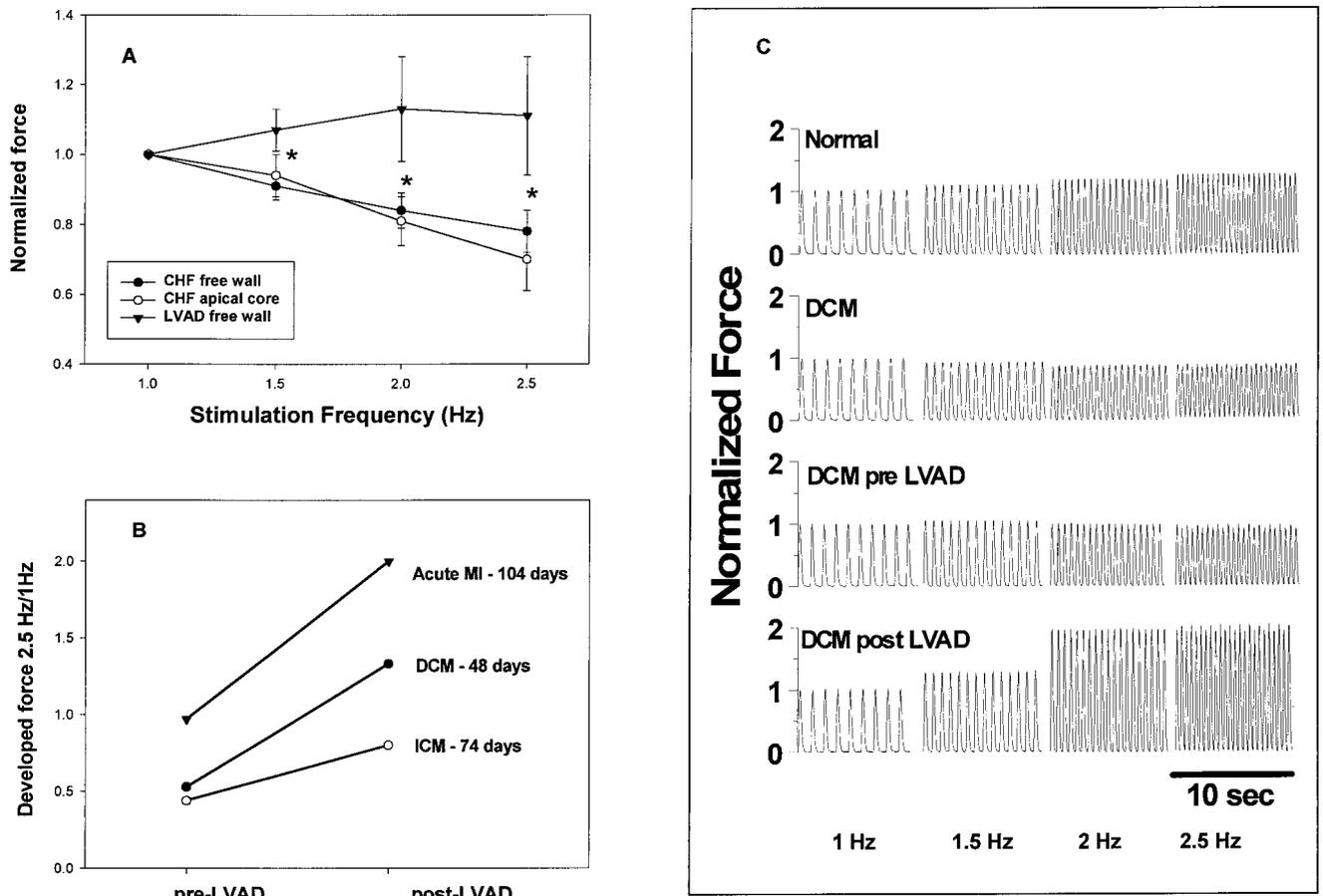
Figure 2. A, Normalized force (mean±SEM) developed at increasing stimulation frequency by isometric LV trabeculae from free wall of failing hearts (CHF free wall, n=15), from apex before LVAD placement (CHF apical core, n=5), and from free wall after LVAD support (LVAD free wall, n=7). *$P \leq 0.05$ for CHF free wall vs LVAD free wall. B, Ratio between force developed at 2.5 and 1 Hz before and after LVAD support in 3 individual hearts. MI indicates myocardial infarction. C, Force tracings from isometrically contracting trabeculae isolated from 1 nonfailing (normal) and 2 DCM hearts. In 1 DCM heart, a negative FFR before LVAD support became markedly positive after LVAD support.

We hypothesized that upregulated expression of genes encoding for proteins involved in Ca^{2+} handling would occur in conjunction with LVAD-induced recovery of force and FFR. Inasmuch as SERCA2a activity has been linked to the FFR, downregulation of the gene encoding for SERCA2a in heart failure[10,12] appears to be associated with the negative FFR. Indeed, recent studies demonstrating that overexpression of SERCA2a in failing human myocytes normalizes their
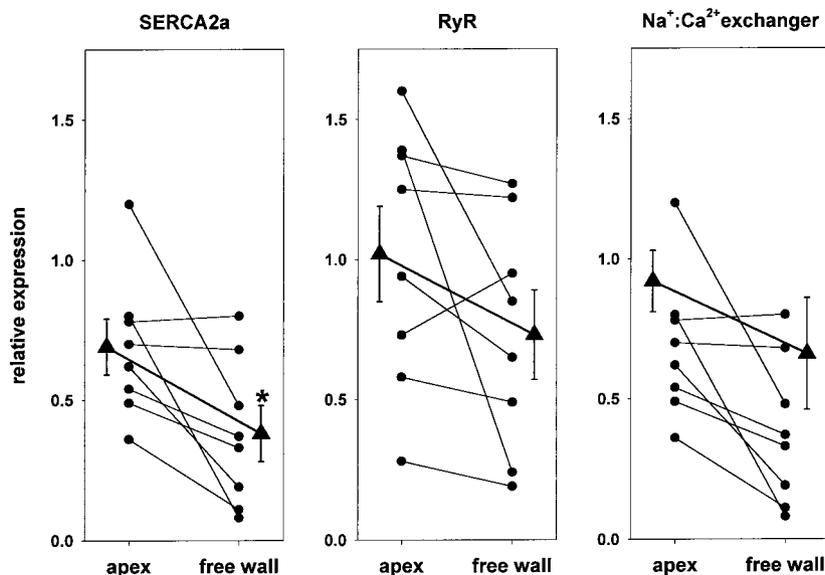

Figure 3. mRNA values from LV apex and free wall of individual CHF patients. Circles represent individual values; triangles, mean±SEM. *$P \leq 0.05$.
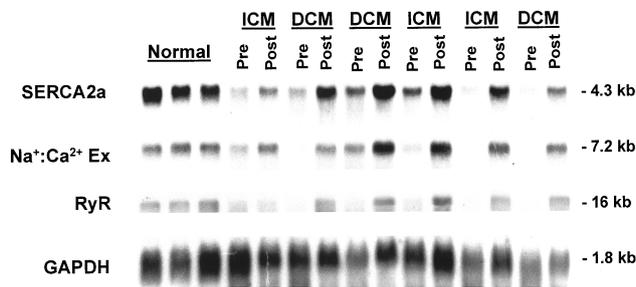
Figure 4. Representative Northern blot depicting 3 nonfailing hearts (normal) and 6 individual hearts before (Pre) and after (Post) LVAD support.

Figure 6. Representative Western blot depicting SERCA2a, RyR, and Na$^+$-Ca^{2+} exchanger (Na$^+$:Ca^{++} Ex) protein in nonfailing (normal) heart along with samples obtained from individual failing hearts before (Pre) and after (Post) LVAD support.

frequency response[23] support functional significance of SERCA2a downregulation. Consistent with these findings, our data suggest that improved force and FFR after LVAD were accompanied by SERCA2a upregulation. Our finding that SERCA2a expression in the apex of non-LVAD hearts was slightly higher than that of the free wall excludes regional heterogeneity as a confounding factor and suggests that the degree of LVAD-induced increase in free wall SERCA2a mRNA may in fact be underestimated. Complementing the gene expression data, the present data also identified a substantial increase in SERCA2a protein levels and increased oxalate-supported Ca^{2+} uptake by isolated SR membranes.

Although the relationship between SERCA2a and FFR has been more extensively studied, properties of the RyR, which
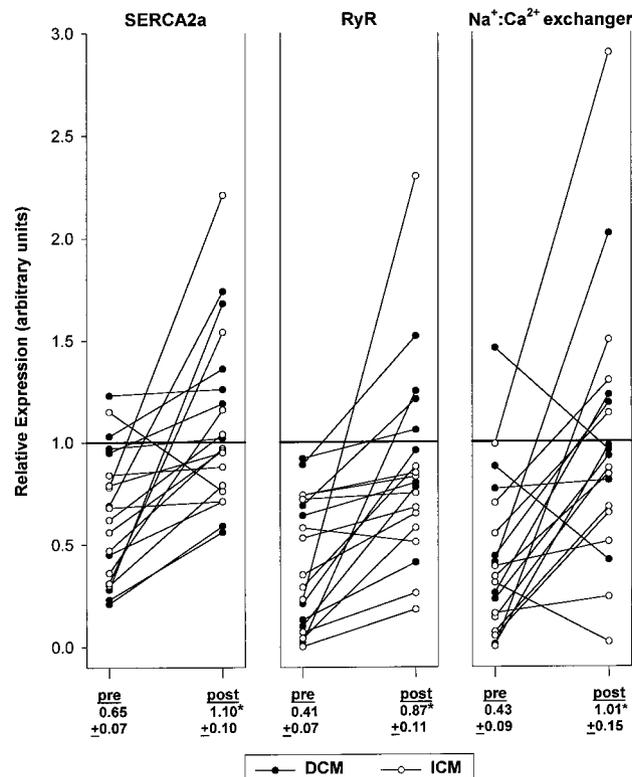
regulates Ca^{2+} release to the myofilaments, also play a pivotal role in the ability of the SR to store and rapidly release Ca^{2+}.[15] We found upregulated expression of the gene encoding for RyR after LVAD support. However, there was little change in the protein content, a finding consistent with the fact that blockade of the RyR with an excess of ryanodine had the same effect on Ca^{2+} uptake by SR membranes isolated from both CHF and CHF+LVAD hearts. In a recent study, we showed that hyperphosphorylation of RyR in failing human myocardium disrupts the normal coupled gating of neighboring receptors, resulting in abnormal ensemble gating patterns, less coordinated SR Ca^{2+} release during excitation, and Ca^{2+} leak during diastole.[21] After LVAD support, these abnormalities are reversed, possibly in response to normalization of the β-adrenergic signaling pathway.[21] Thus, despite subtle changes in gene expression and/or protein content, it appears that channel or pump function may be more affected by posttranslational events.

Results of some studies have indicated that with decreased SERCA2a function in heart failure, a compensatory increase in the activity of the Na$^+$-Ca^{2+} exchanger occurs as this sarcolemmal protein assumes a greater role in extruding Ca^{2+} during diastole.[14,24,25] Consistent with this process are data indicating upregulated myocardial expression of Na$^+$-Ca^{2+} exchanger mRNA in human heart failure.[13] However, recent data indicate that levels of Na$^+$-Ca^{2+} exchanger protein are not necessarily changed in severe human heart failure,[14] and animal studies have suggested that there can be decreased gene expression[26,27] and reduced Ca^{2+} flux through the Na$^+$-Ca^{2+} exchanger in the setting of cardiac failure.[28] Our data show that LVAD support leads to upregulated gene expression but no change in Na$^+$-Ca^{2+} exchanger protein content. Thus, as for RyR, isolated measurement of gene expression may not fully clarify pathophysiological or LVAD-induced changes of the Na$^+$-Ca^{2+} exchanger properties.

In summary, the present data provide evidence that in hearts that have undergone reverse structural remodeling, prolonged LVAD support also produces reverse molecular remodeling and improved myocardial contraction. Our data, in conjunction with other recent reports,[23] suggest that upregulation of SERCA2a in particular may contribute to enhanced contractile function. Although we found increased expression of RyR and Na$^+$-Ca^{2+} genes after LVAD support, protein levels of both were not affected. Thus, their role in the pathophysiology of CHF in general and the effects of LVAD support in particular may be more fully clarified in functional studies that account for posttranslational modification.

Figure 5. mRNA values from pre-LVAD apex and post-LVAD free wall in individual CHF patients, with mean value of 3 nonfailing hearts designated as 1. Open circles represent patients with ICM; closed circles, patients with DCM. Numbers represent mean±SEM. *$P \leq 0.05$.
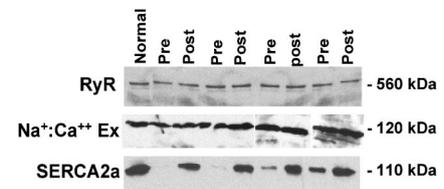
References

1. Levin HR, Oz MC, Chen JM, et al. Reversal of chronic ventricular dilation in patients with end-stage cardiomyopathy by prolonged mechanical unloading. *Circulation*. 1995;91:2717–2720.
2. Frazier OH. First use of an untethered, vented electric left ventricular assist device for long-term support. *Circulation*. 1994;89:2908–2914.
3. Dipla K, Mattiello JA, Jeevanandam V, et al. Myocyte recovery after mechanical circulatory support in humans with end-stage heart failure. *Circulation*. 1998;97:2316–2322.
4. McCarthy PM, Nakatani S, Vargo R, et al. Structural and left ventricular histologic changes after implantable LVAD insertion. *Ann Thorac Surg*. 1995;59:609–613.
5. Altemose GT, Gritsus V, Jeevanandam V, et al. Altered myocardial phenotype after mechanical support in human beings with advanced cardiomyopathy. *J Heart Lung Transplant*. 1997;16:765–773.
6. Levin HR, Oz MC, Catanese KA, et al. Transient normalization of systolic and diastolic function after LVAD support in a patient with dilated cardiomyopathy. *J Heart Lung Transplant*. 1996;15:840–842.
7. Muller J, Wallukat G, Weng YG, et al. Weaning from mechanical cardiac support in patients with idiopathic dilated cardiomyopathy. *Circulation*. 1997;96:542–549.
8. Gomez AM, Valdivia HH, Cheng H, et al. Defective excitation-contraction coupling in cardiac hypertrophy and experimental heart failure. *Science*. 1997;276:800–806.
9. Morgan JP, Erny RE, Allen PD, et al. Abnormal intracellular calcium handling, a major cause of systolic and diastolic dysfunction in ventricular myocardium from patients with heart failure. *Circulation*. 1990;81(suppl III):III-21–III-32.
10. Arai M, Alpert NR, MacLennan DH, et al. Alterations in sarcoplasmic reticulum gene expression in human heart failure: a possible mechanism for alterations in systolic and diastolic properties of the failing myocardium. *Circ Res*. 1993;72:463–469.
11. Go LO, Moschella MC, Watras J, et al. Differential regulation of two types of intracellular calcium release channels during end-stage heart failure. *J Clin Invest*. 1995;95:888–894.
12. Hasenfuss G, Reinecke H, Studer R, et al. Relation between myocardial function and expression of sarcoplasmic reticulum Ca^{2+}-ATPase in failing and nonfailing human myocardium. *Circ Res*. 1994;75:434–442.
13. Studer R, Reinecke H, Bilger J, et al. Gene expression of the cardiac Na^+-Ca^{2+} exchanger in end-stage human heart failure. *Circ Res*. 1994;75:443–453.
14. Hasenfuss G, Schillinger W, Lehnart SE, et al. Relationship between Na^+-Ca^{2+} exchanger protein levels and diastolic function of failing human ventricles. *Circulation*. 1999;99:641–648.
15. Jayaraman T, Brillantes AM, Timerman AP, et al. FK506 binding protein associated with the calcium release channel (ryanodine receptor). *J Biol Chem*. 1992;267:9474–9477.
16. Smart SC, Sagar KB, el Schultz J, et al. Injury to the Ca^{2+} ATPase of the sarcoplasmic reticulum in anesthetized dogs contributes to myocardial reperfusion injury. *Cardiovasc Res*. 1997;36:174–184.
17. Moazami N, Argenziano M, Kohmoto T, et al. Inflow valve regurgitation during left ventricular assist device support may interfere with reverse ventricular remodeling. *Ann Thorac Surg*. 1998;65:628–631.
18. Mancini DM, Beniaminovitz A, Levin H, et al. Low incidence of myocardial recovery in patients with left ventricular assist devices. *Circulation*. 1998;98:2383–2389.
19. Hetzer R, Mueller J, Weng Y, et al. Cardiac recovery in dilated cardiomyopathy by unloading with a left ventricular assist device. *Ann Thorac Surg*. 1999;68:742–749.
20. Zafeiridis A, Jeevanandam V, Houser SR, et al. Regression of cellular hypertrophy after left ventricular assist device support. *Circulation*. 1998;98:656–662.
21. Marx SO, Reiken S, Hisamatsu Y, et al. PKA phosphorylation dissociates FKBP12.6 from the calcium release channel (ryanodine receptor): defective regulation in failing hearts. *Cell*. 2000;101:365–376.
22. Takeishi Y, Jalili T, Hoit BD, et al. Alterations in Ca^{2+} cycling proteins and G alpha q signaling after left ventricular assist device support in failing human hearts. *Cardiovasc Res*. 2000;45:883–888.
23. delMonte F, Harding SE, Schmidt U, et al. Restoration of contractile function in isolated cardiomyocytes from failing human hearts by gene transfer of SERCA2a. *Circulation*. 1999;100:2308–2311.
24. Flesch M, Schwinger RH, Schiffer F, et al. Evidence for functional relevance of an enhanced expression of the Na^+-Ca^{2+} exchanger in failing human myocardium. *Circulation*. 1996;94:992–1002.
25. Litwin SE, Bridge JH. Enhanced Na^+-Ca^{2+} exchange in the infarcted heart: implications for excitation-contraction coupling. *Circ Res*. 1997;81:1083–1093.
26. Yoshiyama M, Takeuchi K, Hanatani A, et al. Differences in expression of sarcoplasmic reticular Ca^{2+}-ATPase and Na^+-Ca^{2+} exchanger genes between adjacent and remote noninfarcted myocardium after myocardial infarction. *J Mol Cell Cardiol*. 1997;29:255–264.
27. Yao A, Su Z, Nonaka A, et al. Abnormal myocyte Ca^{2+} homeostasis in rabbits with pacing-induced heart failure. *Am J Physiol*. 1998;275:H1441–H1448.
28. Dixon IMC, Hata T, Dhalla NS. Sarcolemmal calcium transport in congestive heart failure due to myocardial infarction in rats. *Am J Physiol*. 1992;262:H1387–H1394.